Composite Structures 94 (2012) 1900–1910

Contents lists available at SciVerse ScienceDirect

Composite Structures

journal homepage: www.elsevier.com/locate/compstruct

Assessment of a composite beam finite element based on the proper generalized decomposition

P. Vidal *, L. Gallimard, O. Polit

Laboratoire Energétique, Mécanique, Electromagnétisme, Université Paris Ouest Nanterre-La Défense, 50 rue de Sèvres, 92410 Ville d'Avray, France

ARTICLE INFO

Article history:
Available online 30 December 2011

Keywords:
Finite element method
Beam element
Composite
Proper generalized decomposition

ABSTRACT

In this paper, a finite element based on the Proper Generalized Decomposition (PGD) is presented for the analysis of bi-dimensional laminated beams. The displacement field is approximated as a sum of separated functions of x (axial coordinate) and z (transverse coordinate). This choice yields to an iterative process that consists of computing a product of two one-dimensional functions at each iteration. The capability and the behavior of the PGD approach are shown on isotropic beam with different slenderness ratios. A second and fourth-order expansion with respect to the thickness are considered. Mechanical tests for thin/thick laminated and sandwich beams are presented in order to evaluate the two approaches. They are compared with elasticity and 2D finite element reference solutions.

1. Introduction

Composite and sandwich structures are widely used in the industrial field due to their excellent mechanical properties, especially their high specific stiffness and strength. In this context, they can be subjected to severe mechanical loads. For composite design, accurate knowledge of displacements and stresses is required. So, it is important to take into account effects of the transverse shear deformation due to the low ratio of transverse shear modulus to axial modulus, or failure due to delamination, etc. In fact, they can play an important role on the behavior of structures in services, which leads to evaluate precisely their influence on local stress fields in each layer, particularly on the interface between layers.

According to published research, various theories in mechanics for composite or sandwich structures have been developed. The following classification is associated with the dependancy on the number of degrees of freedom (dofs) with respect to the number of layers:

- The Equivalent Single Layer approach (ESL): the number of unknowns is independent of the number of layers, but the transverse shear and normal stresses continuity on the interfaces between layers are often violated. We can distinguish the classical laminate theory [1] (it is based on the Euler–Bernoulli hypothesis and leads to inaccurate results for composites and moderately thick beams, because both transverse shear and normal strains are neglected), the first order shear deformation theory [2], and higher order theories [3–6]. Some of them take into account transverse normal deformation [7–9] with a higher order theory. All these studies are based on a displacement approach, although other approaches are formulated on the basis of mixed formulations [10,11].
- The Layerwise approach (LW): the number of dofs depends on the number of layers. This theory aims at overcoming the restriction of the ESL concerning the discontinuity of out-of-plane stresses on the interface layers. This approach was introduced in [12,13], and also used in [14–16]. For recent contributions, see [17–19].
  Again, some models which take into account the transverse normal effect have been developed: [20] within a displacement based approach and [21,22,10] within a mixed formulation.

In this framework, refined models have been developed in order to improve the accuracy of ESL models avoiding the additional computational cost of LW approach. Based on physical considerations and after some algebraic transformations, the number of unknowns becomes independent of the number of layers. [15] has extended the work of [23] for symmetric laminated composites with arbitrary orientation and a quadratic variation of the transverse stresses in each layer. So, a family of models, denoted zig-zag models, was derived (see [24–26]). Note also the refined approach based on the Sinus model [27–29]. This above literature deals with only some aspects of the broad research activity about models for layered structures and corresponding finite element formulations. An extensive assessment of different approaches has been made in [30–34].

Over the past years, the Proper Generalized Decomposition (PGD) has shown interesting features in the reduction model

* Corresponding author. Tel./fax: +33 1 40 97 98 23.
E-mail address: philippe.vidal@u-paris10.fr (P. Vidal).

0263-8223/$ - see front matter © 2011 Elsevier Ltd. All rights reserved.
doi:10.1016/j.compstruct.2011.12.016

framework [35]. This type of method has been also introduced by [36] and called "radial approximation" in the Latin method framework. It allows to decrease drastically computational time [37]. It has been also used in the context of separation of coordinate variables in multi-dimensional PDEs [35] and for composite plates in [38]. For a review about the PGD and its fields of applications, the reader can refer to [39,40].

In this work, a finite element based on the PGD for rectangular laminated beam analysis is evaluated. The displacements are written under the form of separated variables representations, i.e. a sum of products of unidimensional polynomials of x and z. The 2D beam is based on a quadratic finite element (FE) approximation for the variation with respect to x. The second and fourth-order LW descriptions are used for the variation with respect to z. Using the PGD, each unknown function of x is classically approximated using one degree of freedom (dof) at the node of the mesh while the LW unknown functions of z are global for the whole beam. Finally, the deduced non-linear problem implies the resolution of two linear problems alternatively. This process yields to few unknowns involved in each of these linear problems.

We now outline the remainder of this article. First the mechanical formulation is given. Then, the FE discretization based on the PGD is described. The principles of the approach are recalled in the framework of our study. It is illustrated by numerical tests which have been performed upon various isotropic, laminated and sandwich beams under a global or localized pressure. This work deals with the monomial terms in the z expansion and the mode (functions of x) which are involved in the displacement, depending on the boundary conditions and the stacking sequences of the beam. A special attention is pointed towards the behavior of the PGD process to build these modes. A comparison between two LW descriptions in the thickness (second and fourth-order) is given. The accuracy of the results are evaluated by comparisons with an exact three-dimensional theory for laminates in bending [16] and also two-dimensional finite element computations using commercial finite element software. Finally, the most accurate model is assessed on a highly anisotropic sandwich beam.

2. Reference problem description

2.1. The governing equations

Let us consider a beam occupying the domain $\mathcal{B} = \mathcal{B}_x \times \mathcal{B}_z \times \left[-\frac{b}{2} \leqslant y \leqslant \frac{b}{2}\right] = [0, L] \times \left[-\frac{h}{2} \leqslant z \leqslant \frac{h}{2}\right] \times \left[-\frac{b}{2} \leqslant y \leqslant \frac{b}{2}\right]$ in a Cartesian coordinate (x,y,z). The beam has a rectangular uniform cross section of height h, width b and is assumed to be straight. The beam is made of NC layers of different linearly elastic materials. Each layer may be assumed to be orthotropic in the beam axes. The x axis is taken along the central line of the beam whereas y and z are the two axes of symmetry of the cross section intersecting at the centroid, see Fig. 1. As shown in this figure, the y axis is along the width of the beam. This work is based upon a displacement approach for geometrically linear elastic beams.

In the following, the beam is considered in the (x,z) plane, the y-coordinate is neglected.

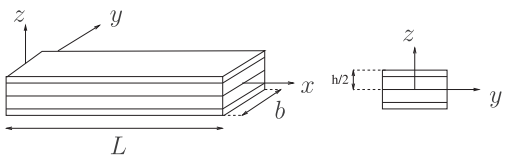

Fig. 1. The laminated beam and co-ordinate system.

2.1.1. Constitutive relation

Each layer of the laminate is assumed to be orthotropic. Using matrix notation, the stress–strain law of the kth layer is given by:

$$\begin{bmatrix} \sigma_{11}^{(k)} \\ \sigma_{33}^{(k)} \\ \sigma_{13}^{(k)} \end{bmatrix} = \begin{bmatrix} \overline{C}_{11}^{(k)} & \overline{C}_{13}^{(k)} & 0 \\ & \overline{C}_{33}^{(k)} & 0 \\ symm & & \overline{C}_{55}^{(k)} \end{bmatrix} \begin{bmatrix} \varepsilon_{11}^{(k)} \\ \varepsilon_{33}^{(k)} \\ \varepsilon_{13}^{(k)} \end{bmatrix} \text{ i.e. } [\sigma^{(k)}] = [\overline{C}^{(k)}][\varepsilon^{(k)}] \tag{1}$$

where we denote the stress tensor $[\sigma]$ and the strain tensor $[\varepsilon]$. $\overline{C}_{ij}^{(k)}$ are the moduli of the material for the kth layer taking into account the zero transverse normal stress hypothesis ($\sigma_{22} = 0$). They are expressed by

$$\overline{C}_{ij}^{(k)} = C_{ij}^{(k)} - C_{i2}^{(k)} C_{j2}^{(k)} / C_{22}^{(k)} \tag{2}$$

where $C_{ij}^{(k)}$ are orthotropic three-dimensional elastic moduli. We also have $\overline{C}_{55}^{(k)} = C_{55}^{(k)}$.

2.1.2. The weak form of the boundary value problem

Using the above matrix notation and for admissible displacement $\delta\vec{u} \in \delta U$, the variational principle is given by: find $\vec{u} \in U$ (space of admissible displacements) such that

$$\begin{aligned} &-\int_{\mathcal{B}} [\varepsilon(\delta\vec{u})]^T [\sigma(\vec{u})] d\mathcal{B} + \int_{\mathcal{B}} [\delta u]^T [b] d\mathcal{B} + \int_{\partial\mathcal{B}_F} [\delta u]^T [F] d\partial\mathcal{B} = 0 \\ &\forall \delta\vec{u} \in \delta U \end{aligned} \tag{3}$$

where $[b]$ and $[F]$ are the prescribed body and surface forces applied on $\partial\mathcal{B}_F$.

2.2. The displacement field for the composite beam

In classical beam theory, the displacement field is assumed to be of the following form

$$u_1(x,z) = \sum_{i=0}^{N_1} z^i v_1^i(x) \tag{4}$$

$$u_3(x,z) = \sum_{i=0}^{N_3} z^i v_3^i(x) \tag{5}$$

where (v_1^i, v_3^i) are the functions to be sought.

For instance, we can derive two models available in the literature:

- the classical Timoshenko model with $N_1 = 1$ and $N_3 = 0$,
- ED2 model in Carrera's Unified Formulation [32] with $N_1 = N_3 = 2$.

3. Application of the proper generalized method to beam

The Proper Generalized Decomposition (PGD) was introduced in [35] and is based on an *a priori* construction of separated variables representation of the solution. In this section, we briefly introduce the PGD for beam analysis.

3.1. The displacement and the strain field

The displacement solution $(u_1(x,z), u_3(x,z))$ is constructed as the sum of N products of functions of only one spatial coordinate ($N \in \mathbb{N}$ is the order of the representation)

$$u = \begin{pmatrix} u_1(x,z) \\ u_3(x,z) \end{pmatrix} = \sum_{i=1}^{N} \begin{pmatrix} f_1^i(z) v_1^i(x) \\ f_3^i(z) v_3^i(x) \end{pmatrix} \tag{6}$$

where (f_1^i, f_3^i) are defined in $\mathcal{B}_z$ and (v_1^i, v_3^i) are defined in $\mathcal{B}_x$. In this paper, a classical quadratic FE approximation is used in $\mathcal{B}_x$ and a LW description is chosen in $\mathcal{B}_z$ as it is particulary suitable for the modeling of composite structure. The strain derived from Eq. (6) is

$$\varepsilon(u) = \sum_{i=1}^{N} \begin{pmatrix} f_1^i (v_1^i)' \\ (f_3^i)' v_3^i \\ (f_1^i)' v_1^i + f_3^i (v_3^i)' \end{pmatrix} \tag{7}$$

3.2. The problem to be solved

For sake of clarity the surfaces forces are neglected in the developments and the weak form of the beam problem introduced in Eq. (3) simplifies in

$$-\int_{\mathcal{B}_x}\int_{\mathcal{B}_z} ([\varepsilon(\delta u)]^T[C][\varepsilon(u)] + [\delta u]^T[b])\, dz\, dx = [0] \tag{8}$$

where $[C]$ represents, in each layer (k), the matrix of the elastic moduli.

Following the approach proposed in [35], Eq. (8) is solved by an iterative procedure. If we assume that the first n functions have been already computed, the trial function for the iteration $n+1$ is written as

$$u^{n+1} = \bar{u} + \begin{pmatrix} f_1 v_1 \\ f_3 v_3 \end{pmatrix} \tag{9}$$

where (v_1, v_3), (f_1, f_3) are the functions to be computed and $\bar{u}$ is the associated known set at iteration n defined by

$$\bar{u} = \sum_{i=1}^{n} \begin{pmatrix} f_1^i v_1^i \\ f_3^i v_3^i \end{pmatrix} \tag{10}$$

The test function is

$$\delta \begin{pmatrix} f_1 v_1 \\ f_3 v_3 \end{pmatrix} = \begin{pmatrix} \delta f_1 v_1 + f_1 \delta v_1 \\ \delta f_3 v_3 + f_3 \delta v_3 \end{pmatrix} = \mathbf{V}\delta f + \mathbf{F}\delta v \tag{11}$$

where

$$v = \begin{pmatrix} v_1 \\ v_3 \end{pmatrix} \quad f = \begin{pmatrix} f_1 \\ f_3 \end{pmatrix} \quad \mathbf{V} = \begin{pmatrix} v_1 & 0 \\ 0 & v_3 \end{pmatrix} \quad \mathbf{F} = \begin{pmatrix} f_1 & 0 \\ 0 & f_3 \end{pmatrix} \tag{12}$$

The test function defined by Eq. (11) and the trial function defined by Eq. (9) are introduced into the weak form (Eq. (8)) to obtain two equations

$$\begin{aligned} &\int_{\mathcal{B}_x}\int_{\mathcal{B}_z} ([\varepsilon(\mathbf{F}\delta v)]^T[C][\varepsilon(\mathbf{F}v)])\, dz\, dx \\ &\quad = \int_{\mathcal{B}_x}\int_{\mathcal{B}_z} ([\mathbf{F}\delta v]^T[b] - [\varepsilon(\mathbf{F}\delta v)]^T[C][\varepsilon(\bar{u})])\, dz\, dx \end{aligned} \tag{13}$$

$$\begin{aligned} &-\int_{\mathcal{B}_x}\int_{\mathcal{B}_z} ([\varepsilon(\mathbf{V}\delta f)]^T[C][\varepsilon(\mathbf{V}f)])\, dz\, dx \\ &\quad = -\int_{\mathcal{B}_x}\int_{\mathcal{B}_z} ([\varepsilon(\mathbf{V}\delta f)]^T[C][\varepsilon(\bar{u})] + [\mathbf{V}\delta f]^T[b])\, dz\, dx \end{aligned} \tag{14}$$

As these equations define a coupled non-linear problem, a non-linear resolution strategy has to be used. The simplest strategy is a fixed point method. An initial function $f^{(0)}$ is set, and at each step, the algorithm computes a new pair $(v^{(m+1)}, f^{(m+1)})$ such that

- $v^{(m+1)}$ satisfies Eq. (13) for f set to $f^{(m)}$
- $f^{(m+1)}$ satisfies Eq. (14) for v set to $v^{(m+1)}$

These two equations are linear and the first one is solved on $\mathcal{B}_x$, while the second one is solved on $\mathcal{B}_z$. The fixed point algorithm is stopped when

$$\sqrt{\int_{\mathcal{B}_x}\int_{\mathcal{B}_z} \left(v_1^{(m+1)} f_1^{(m+1)} - v_1^{(m)} f_1^{(m)}\right)^2 + \left(v_3^{(m+1)} f_3^{(m+1)} - v_3^{(m)} f_3^{(m)}\right)^2 dx\, dz} \leqslant \varepsilon \tag{15}$$

where ε is a parameter to be fixed by the user. In this paper we set $\varepsilon = 10^{-6}$.

3.3. Finite element discretization

To build the beam finite element approximation, a discrete representation of the functions (v,f) must be introduced. We use a classical finite element approximation in $\mathcal{B}_x$, and a polynomial expansion in $\mathcal{B}_z$. The elementary vector of degree of freedom (dof) associated with the finite element mesh in $\mathcal{B}_x$ is denoted $[q_e^v]$ and the vector of dof associated with the polynomial expansion in $\mathcal{B}_z$ is denoted $[q^f]$. The displacement fields and the strain fields are determined from the values of $[q_e^v]$ and $[q^f]$ by

$$v_e = [\mathbf{N}_x][q_e^v],\ [\mathcal{E}_v^e] = [\mathbf{B}_x][q_e^v],\ f = [\mathbf{N}_z][q^f] \text{ and } [\mathcal{E}_f] = [\mathbf{B}_z][q^f] \tag{16}$$

The matrix $[\mathbf{N}_x]$, $[\mathbf{B}_x]$, $[\mathbf{N}_z]$, $[\mathbf{B}_z]$ contain the interpolation functions, their derivatives and the jacobian components dependent on the chosen discrete representation.

3.4. Finite element problem to be solved on $\mathcal{B}_x$

For the sake of simplicity, the function $f^{(m)}$ which is assumed to be known, will be denoted $\bar{f}$ (and $\bar{\mathbf{F}}$), and the function $v^{(m+1)}$ to be computed will be denoted v. The strain in Eq. (13) is defined in matrix notations as

$$[\varepsilon(\bar{\mathbf{F}}v)] = [\mathbf{B}_z(\bar{f})][\mathcal{E}_v] \tag{17}$$

with

$$[\mathbf{B}_z(\bar{f})] = \begin{bmatrix} 0 & \bar{f}_1 & 0 & 0 \\ 0 & 0 & \bar{f}_3' & 0 \\ \bar{f}_1' & 0 & 0 & \bar{f}_3 \end{bmatrix} \text{ and } [\mathcal{E}_v] = \begin{bmatrix} v_1 \\ v_1' \\ v_3 \\ v_3' \end{bmatrix} \tag{18}$$

The variational problem defined on $\mathcal{B}_x$ from Eq. (13) is

$$\begin{aligned} \int_{\mathcal{B}_x} [\delta\mathcal{E}_v]^T[k_z(\bar{f})][\mathcal{E}_v]dx &= \int_{\mathcal{B}_x} [\delta v]^T[f_z(\bar{f})]dx \\ &\quad - \int_{\mathcal{B}_x} [\delta\mathcal{E}_v]^T[\sigma_z(\bar{f},\bar{u})]dx \end{aligned} \tag{19}$$

with

$$[k_z(\bar{f})] = \int_{\mathcal{B}_z} [\mathbf{B}_z(\bar{f})]^T[C][\mathbf{B}_z(\bar{f})]dz \tag{20}$$

$$[f_z(\bar{f})] = \int_{\mathcal{B}_z} [\bar{\mathbf{F}}]^T[b]dz \tag{21}$$

$$[\sigma_z(\bar{f},\bar{u})] = \int_{\mathcal{B}_z} [\mathbf{B}_z(\bar{f})]^T[C][\varepsilon(\bar{u})]dz \tag{22}$$

The introduction of the finite element approximation (16) in the variational Eq. (19) leads to the linear system

$$[\mathbf{K}_z(\bar{f})][\mathbf{q}^v] = \mathcal{R}_v(\bar{f},\bar{u}) \tag{23}$$

where $[\mathbf{q}^v]$ is the vector of the nodal displacements associated with the finite element mesh in $\mathcal{B}_x$, $[\mathbf{K}_z(\bar{f})]$ the stiffness matrix obtained by summing the elements' stiffness matrices $[\mathbf{K}_z^e(\bar{f})]$ and $[\mathcal{R}_v(\bar{f},\bar{u})]$ the equilibrium residual obtained by summing the elements' residual load vectors $[\mathcal{R}_v^e(\bar{f},\bar{u})]$

$$[\mathbf{K}_z^e(\bar{f})] = \int_{L_e} [\mathbf{B}_x]^T[k_z(\bar{f})][\mathbf{B}_x]dx \tag{24}$$

and

$$[\mathcal{R}_v^e(\bar{f},\bar{u})] = \int_{L_e} [\mathbf{N}_x]^T[f_z(\bar{f})]dx - \int_{L_e} [\mathbf{B}_x]^T[\sigma_z(\bar{f},\bar{u})]dx \tag{25}$$

3.5. Finite element problem to be solved on $\mathcal{B}_z$

For the sake of simplicity, the function $v^{(m+1)}$ which is assumed to be known, will be denoted $\bar{v}$ (and $\overline{\mathbf{V}}$), and the function $f^{(m+1)}$ to be computed will be denoted f. The strain in Eq. (14) is defined in matrix notations as

$$[\varepsilon(\overline{\mathbf{V}}f)] = [\mathbf{B}_x(\bar{v})][\mathcal{E}_f] \tag{26}$$

with

$$[\mathbf{B}_x(\bar{v})] = \begin{bmatrix} \bar{v}_1' & 0 & 0 & 0 \\ 0 & 0 & 0 & \bar{v}_3 \\ 0 & \bar{v}_1 & \bar{v}_3' & 0 \end{bmatrix} \text{ and } [\mathcal{E}_f] = \begin{bmatrix} f_1 \\ f_1' \\ f_3 \\ f_3' \end{bmatrix} \tag{27}$$

The variational problem defined on $\mathcal{B}_z$ from Eq. (14) is

$$\int_{\mathcal{B}_z} [\delta\mathcal{E}_f]^T [k_x(\bar{v})][\mathcal{E}_f]dx = \int_{\mathcal{B}_z} [\delta F]^T [f_x(\bar{v})]dx - \int_{\mathcal{B}_z} [\delta\mathcal{E}_f]^T [\sigma_x(\bar{v},\bar{u})]dz \tag{28}$$

with

$$[k_x(\bar{v})] = \int_{\mathcal{B}_x} [\mathbf{B}_x(\bar{v})]^T [C][\mathbf{B}_x(\bar{v})]dx \tag{29}$$

$$[f_x(\bar{v})] = \int_{\mathcal{B}_x} [\overline{\mathbf{V}}]^T [b]dx \tag{30}$$

$$[\sigma_x(\bar{v},\bar{u})] = \int_{\mathcal{B}_x} [\mathbf{B}_x(\bar{v})]^T [C][\varepsilon(\bar{u})]dz \tag{31}$$

The introduction of the finite element discretization (16) in the variational Eq. (28) leads to the linear system

$$[\mathbf{K}_x(\bar{v})][\mathbf{q}^f] = [\mathcal{R}_f(\bar{v},\bar{u})] \tag{32}$$

where $[\mathbf{q}^f]$ is the vector of degree of freedom associated with the polynomial expansion in $\mathcal{B}_z$, $[\mathbf{K}_x(\bar{v})]$ is a stiffness matrix defined by (33) and $[\mathcal{R}_f(\bar{v},\bar{u})]$ an equilibrium residual defined by (34)

$$[\mathbf{K}_x(\bar{v})] = \int_{\mathcal{B}_z} [\mathbf{B}_z]^T [k_x(\bar{v})][\mathbf{B}_z]dx \tag{33}$$

$$[\mathcal{R}_f(\bar{v},\bar{u})] = \int_{\mathcal{B}_z} [\mathbf{N}_z]^T [f_x(\bar{v})]dz - \int_{\mathcal{B}_z} [\mathbf{B}_z]^T [\sigma_x(\bar{v},\bar{u})]dz \tag{34}$$

4. Numerical results

In this section, several static tests are presented validating our approach, evaluating its efficiency and showing the properties of the algorithm. A classical quadratic finite element is used for the unknowns depending on the x-axis coordinate. For the transverse direction, a quadratic and fourth-order layer-wise description is chosen. The present models are herein denoted by the acronym B2LD2-PGD and B2LD4-PGD respectively as a reference to the nomenclature from [32]. B2 refers to the quadratic Beam FE, LDN means Layer-Wise approach in a Displacement formulation with a Nth order expansion in z.

First, the behavior of the approach is shown on an isotropic beam submitted to a localized load. An interesting feature of the method is the capability to give the utmost terms of the expansion with respect to the z-coordinate. Then, a comparison between the second and fourth-order LW description is addressed. Finally, the most accurate model is assessed on the flexural behavior of a highly anisotropic sandwich beam.

For all these tests, the numbers of dofs are also precised for the two problems associated with (v_1^i, v_3^i) and (f_1^i, f_3^i). They are denoted $Ndof_x$ and $Ndof_z$ respectively.

Note that the convergence rate of the fixed point process is high. Usually, only less than four iterations are required. This subject is not discussed here.

4.1. Properties of the PGD: bending analysis of isotropic beam under localized pressure

This test is about clamped–clamped isotropic beam submitted to a localized pressure. We focus on the behavior of the approach on a quite severe test and its capability to capture local effects. It is shown in Fig. 2 and detailed below:

Geometry: $S = \frac{L}{h} = 4$
Boundary conditions: clamped–clamped beam subjected to a transverse pressure $q(x_1) = q_0$ applied on a line of length $L_p = L/8$ at the beam center (see Fig. 2).
Material properties: $E = 10^6$ MPa, $\nu = 0.3$
Mesh: N_x=16, half of the beam is meshed.
Model: B2LD4-PGD
Results: The reference solution is issued from a 2D elasticity analysis with a very refined mesh including 7000 dofs in ANSYS. The element PLANE82 is used.

Figs. 3 and 4 give the distribution of the transverse displacement, in-plane, transverse shear and normal stresses through the thickness.These figures show the evolution of the solution for different number of couples in the PGD process. For this thick beam, six couples are necessary to obtain a very good agreement with the 2D reference solution for both displacements and stresses. For each couple, the shape functions in the thickness $f_1^i(z)/f_3^i(z)$ and along the x-axis $v_1^i(x)/v_3^i(x)$ are given in Figs. 5 and 6 respectively. As the solution is the product $f_1^i(z)v_1^i(x)$ (Figs. 5 and 6 left) for the axial displacement and $f_3^i(z)v_3^i(x)$ (Figs. 5 and 6 right) for the transverse one, the following comments can be made:

- The first solution calculated with the first couple corresponds to the Timoshenko model, i.e. a linear and constant variation through the thickness for the axial and the transverse displacements respectively.
- The four following modes can be considered as a local correction of the first global solution. A high gradient appears near the clamped edge and the localized pressure.
- The last couple represents a global mode.
- All the terms $f_1^i(z)$–$f_3^i(z)$ are normalized. So, the maximum value of each term $v_1^i(x)$–$v_3^i(x)$ in Fig. 6 gives the order of magnitude of each correction. It confirms that the main mode is the first one.
- Finally, the interesting feature of the method is its capability to build complex shape functions depending on the problem to be solved.

Note that an orthogonalization of the modes is not used, and the optimization of the z-functions $f_1^i(z)$–$f_3^i(z)$ with the known axial basis is not carried out.

Moreover, the approach allows us to deduce the utmost terms in the z-expansion for the axial and transverse displacements. Figs. 7 and 8 show the influence of the slenderness ratio. For

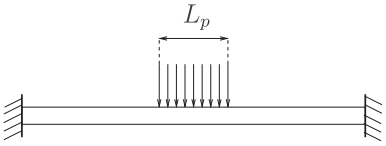

Fig. 2. Beam under localized pressure.

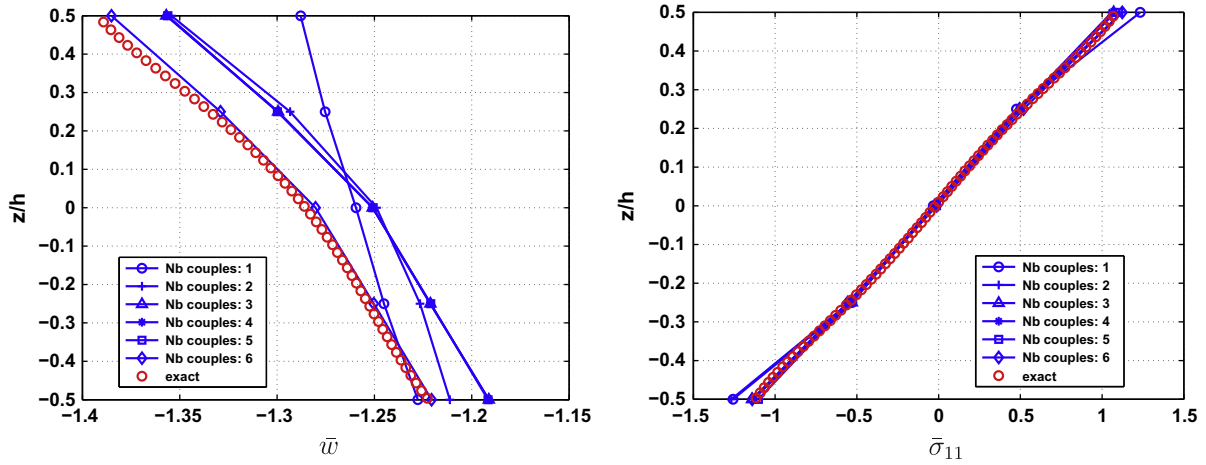

Fig. 3. Distribution of $\bar{w}$ (left) and $\bar{\sigma}_{11}$ (right) along the thickness for different number of couples – $S = 4$ – isotropic-localized pressure – B2LD4-PGD.

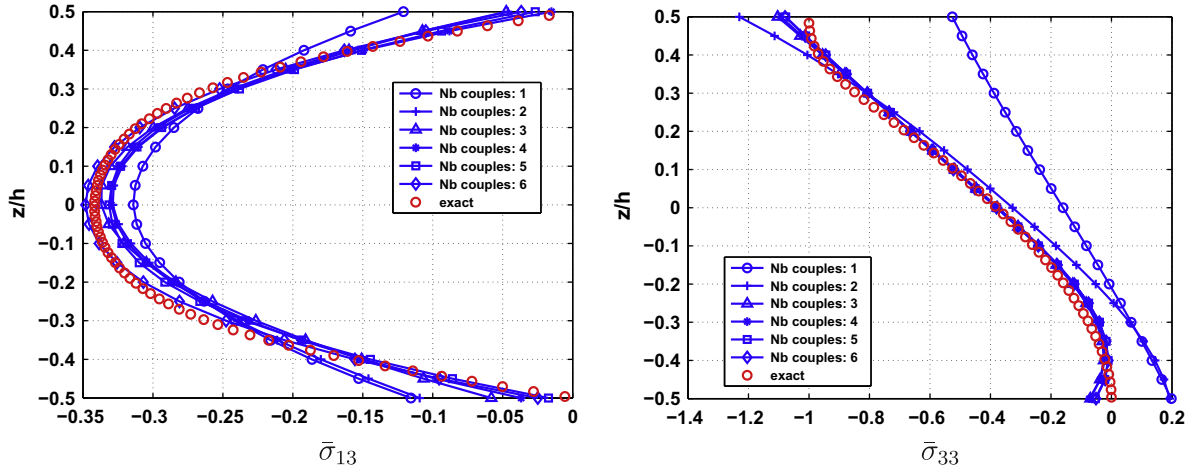

Fig. 4. Distribution of $\bar{\sigma}_{13}$ (left) and $\bar{\sigma}_{33}$ (right) along the thickness for different number of couples – $S = 4$ – isotropic-localized pressure – B2LD4-PGD.

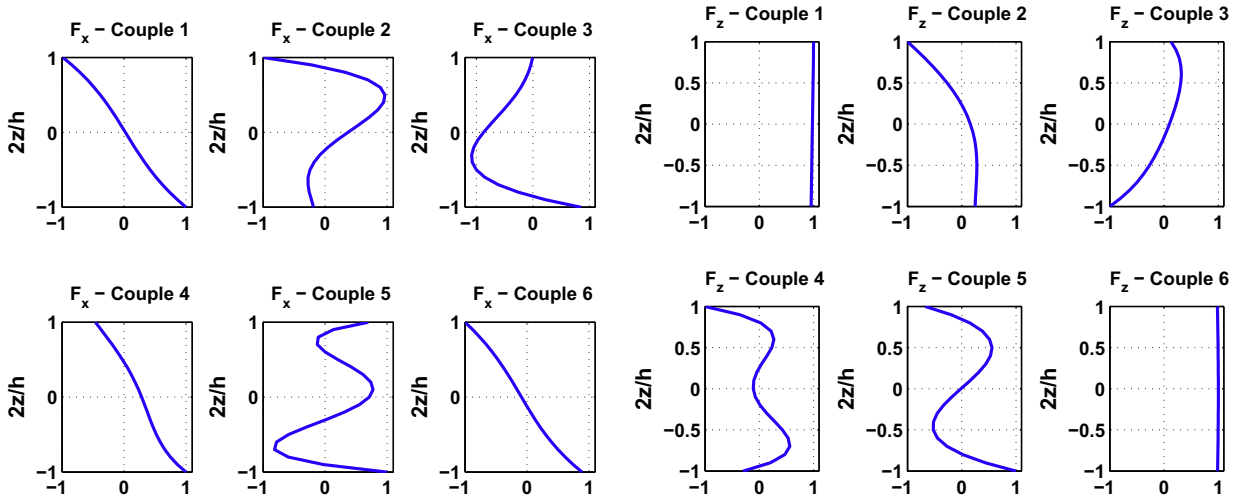

Fig. 5. $f_1^i(z)$ (left)/$f_3^i(z)$ (right) – $S = 4$ – isotropic-localized pressure – B2LD4-PGD.

the thick structure, all the terms in the fourth-order expansion are needed. For the thin structure, the axial displacement requires only the 1st and 3rd terms. For the deflection, only the constant, 2nd, 4th terms are active. The representation of the first function in Fig. 8 confirms that it corresponds to the Timoshenko model. This knownledge is interesting in the framework of advanced models based on *a priori* assumptions in the kinematics.

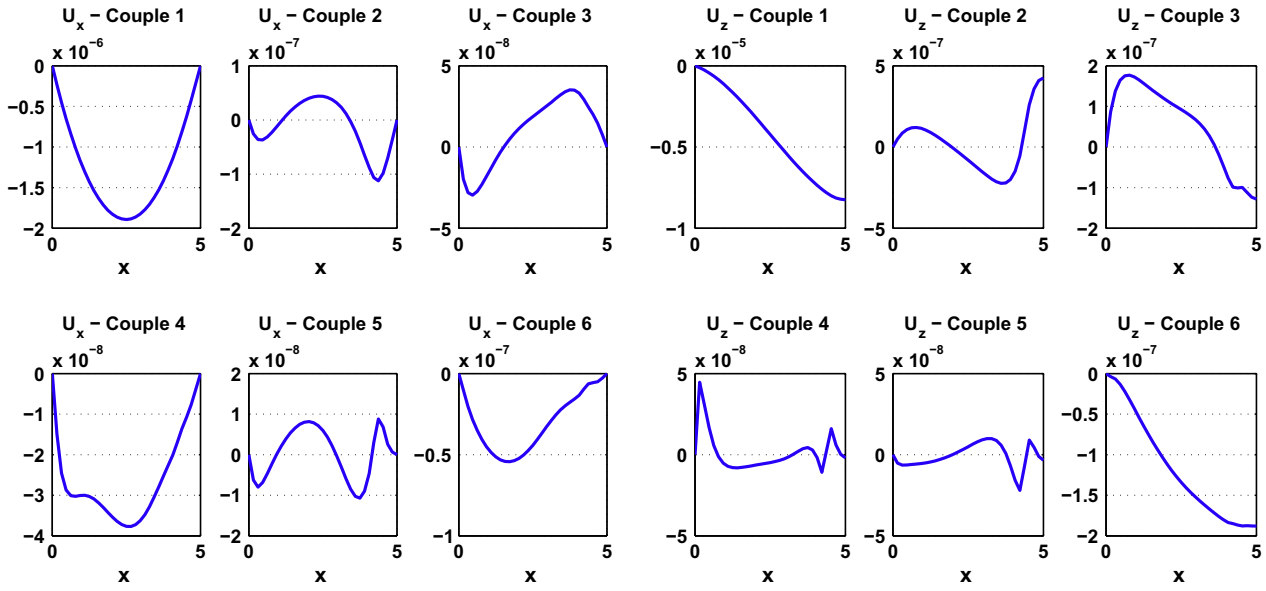

Fig. 6. $v_1^i(x)$ (left)/$v_3^i(x)$ (right) – $S = 4$ – isotropic-localized pressure – B2LD4-PGD.

4.2. Comparison between B2LD2-PGD and B2LD4-PGD

In this section, the B2LD2-PGD and B2LD4-PGD approaches are compared. The bending analysis of symmetric and antisymmetric laminated composite beam is considered. The results are given for very thick and thin structures to see the influence of the slenderness ratio. The configurations are detailed below:

Geometry: composite cross-ply beam (0°/ 90°), (0°/90°/0°) and length-to-thickness ratio $S = 2/4/20/40/100$. All layers have the same thickness.
Boundary conditions: simply supported beam subjected to sinusoidal load $q(x) = q_0 \sin\frac{\pi x}{L}$.
Material properties:

$$E_L = 172.4\ \text{GPa},\ E_T = 6.895\ \text{GPa},\ G_{LT} = 3.448\ \text{GPa},$$
$$G_{TT} = 1.379\ \text{GPa},\ \nu_{LT} = \nu_{TT} = 0.25$$

where L refers to the fiber direction, T refers to the transverse direction.

Mesh: half of the beam is meshed. $N_x = 8$ with spacing ratio (6) (denoted sr (6)), $\frac{L_{e\ max}}{L_{e\ min}} = 6$, where $L_{e\ max}$ and $L_{e\ min}$ are the maximal and minimal length of the elements. The mesh is refined near the two edges of the finite element model.
Number of dofs: $Ndof_x = 32$ and $Ndof_z = 4 \times NC + 2$(B2LD2-PGD), $Ndof_z = 8 \times NC + 2$ (B2LD4-PGD)
Results: The results $(\bar{u}, \bar{w}, \bar{\sigma}_{11}, \bar{\sigma}_{13})$ are made non-dimensional using:

$$\bar{u} = u_1(0, h/2)\frac{E_T}{hq_0} \quad \bar{w} = u_3(L/2, 0)\frac{100E_T}{S^4 hq_0}$$
$$\bar{\sigma}_{ij} = \sigma_{ij}\frac{1}{q_0} \text{ for } \begin{cases} \sigma_{11}(L/2, h/2) \\ \sigma_{13}(0, 0) \end{cases} \tag{35}$$

The exact solution of the beam problem is derived from [16].

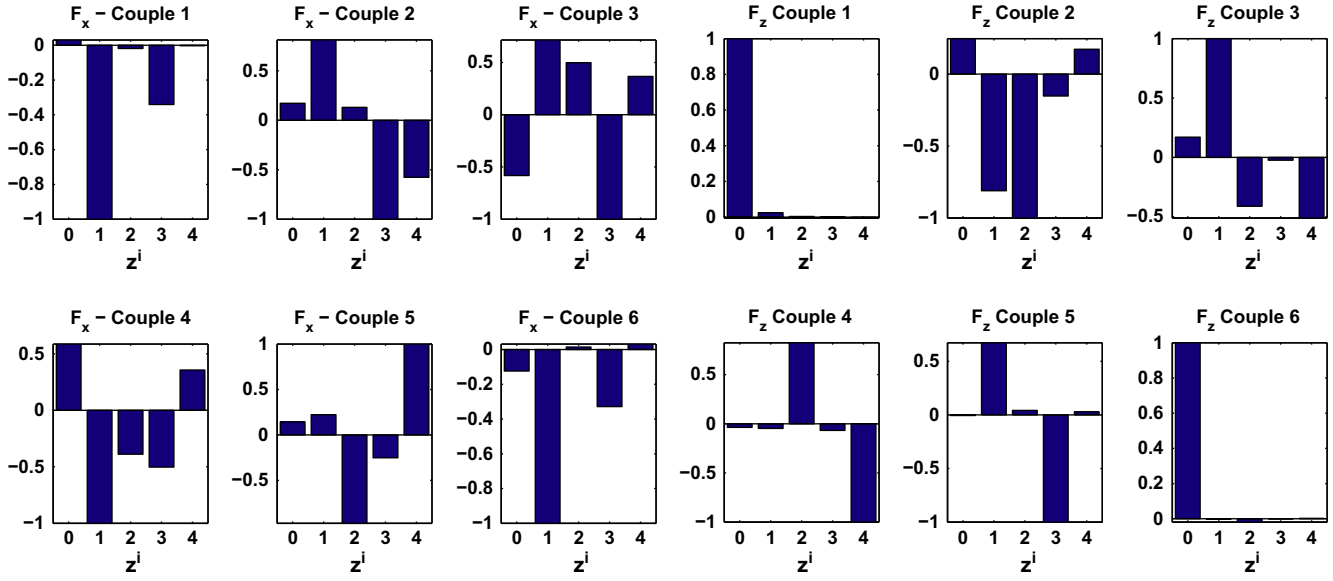

Fig. 7. Values of each term of the z-expansion in $f_1^i(z)$ (left)/$f_3^i(z)$ (right) – $S = 4$ – isotropic-localized pressure – B2LD4-PGD.

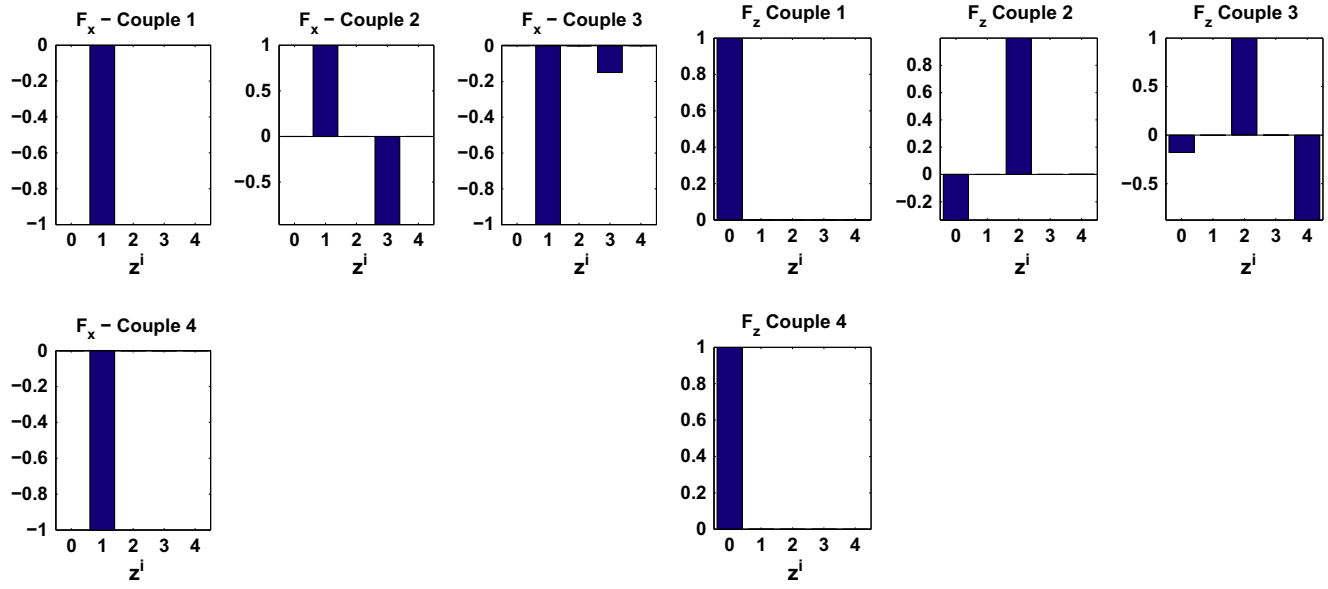

Fig. 8. Values of each term of the z-expansion in $f_1^i(z)/f_3^i(z)$ – $S = 100$ – isotropic-localized pressure – B2LD4-PGD.

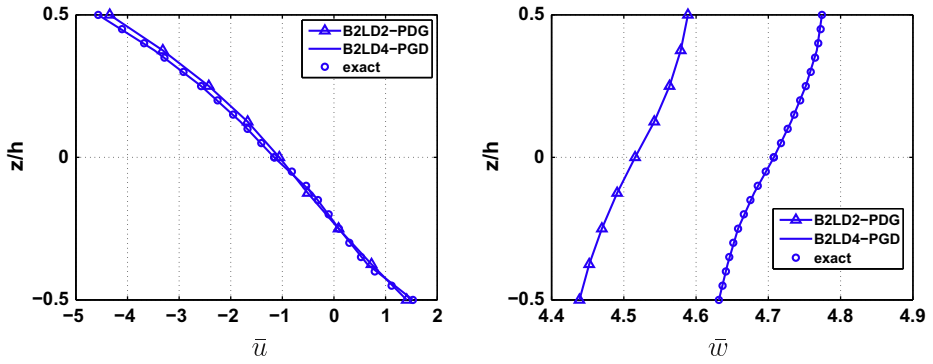

Fig. 9. Distribution of $\bar{u}$ (left) and $\bar{w}$ (right) along the thickness – $S = 4$ – 2 layers (0°/90°) – $N_z = NC$.

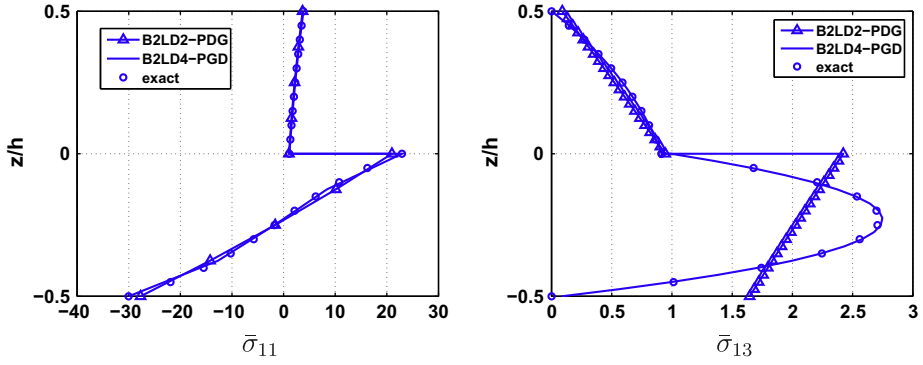

Fig. 10. Distribution of $\bar{\sigma}_{11}$ (left) and $\bar{\sigma}_{13}$ (right) along the thickness – $S = 4$ – 2 layers (0°/90°) – $N_z = NC$.

The two approaches based on a second-order (B2LD2-PGD) and a fourth-order (B2LD4-PGD) expansion are compared in Figs. 9–14 for symmetric and antisymmetric composite beam. As the boundary conditions are not severe, only one couple is built. The results of B2LD4-PGD are in excellent agreement with the exact solution for both the displacements and stresses. The B2LD2-PGD model gives quite similar results for the displacements and the axial stress. For the transverse shear and the normal stresses, a fourth-order approach is necessary to recover accurate results. In fact, a linear variation per layer of the transverse shear stress occurs for the B2LD2-PGD. As far as the transverse normal stress is concerned, a discontinuity appears with this model.

Numerical results from B2LD4-PGD are summarized in Tables 1 and 2 for a large range of length-to-thickness ratios. Note that the

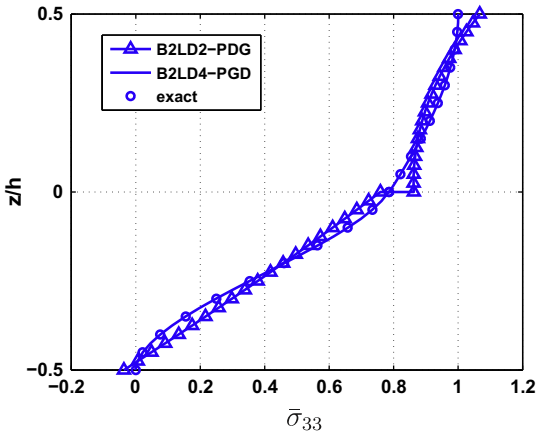

Fig. 11. Distribution of $\bar{\sigma}_{33}$ along the thickness – $S = 4$ – 2 layers (0°/90°) – $N_z = NC$.

model performs very well with respect to the exact solution, except for the transverse shear stress for a very thin beam. As it has been noticed in [41], it is necessary to refine the mesh to improve the accuracy of this one. It is due to the quadratic FE interpolation for all the components of the displacements. Fig. 15 shows the effect of the slenderness ratio on the convergence. For $S = 100$, a regular mesh with $N_x = 32$ is necessary to have an error rate of 1% for the transverse shear and normal stresses. For $S = 4$, the error is lower with a coarse mesh.

4.2.1. Bending analysis of a sandwich beam under a sinusoidal pressure

A sandwich beam under a sinusoidal pressure with a high value of face-to-core stiffness ratio is presented. This severe test allows us to evaluate the capability of the model for a high anisotropy. This case has already been studied in [42].

This example is detailed now.

Geometry: The 3-layer sandwich beam has aluminum alloy faces and a soft core with thickness 0.1 h/0.8 h/0.1 h and length-to-thickness ratio $S = 4$; half of the beam is meshed
Boundary conditions: simply supported beam under a sinusoidal pressure $q(x) = q_0 \sin\left(\frac{\pi x}{L}\right)$
Material properties: Face: $E_f = 73000$ MPa, $\nu = 0.34$.
Core: $E_c = \eta E_f$, with $\eta = 10^{-5}$
Mesh: $N_x = 16$ sr (8)
Number of dofs: $Ndof_x = 64$ and $Ndof_z = 26$
Model: B2LD4-PGD
Results: the results $(\bar{u}, \bar{w}, \bar{\sigma}_{11}, \bar{\sigma}_{13})$ are made non-dimensional using:

$$\bar{u} = \frac{E_f u_1(0,-h/2)}{h q_0} \quad \bar{w} = \frac{100 E_f u_3(L/2,0)}{S^4 h q_0}$$
$$\bar{\sigma}_{11} = \frac{\sigma_{11}(L/2,-h/2)}{q_0} \quad \bar{\sigma}_{13} = \frac{\sigma_{13}(0,0)}{q_0} \tag{36}$$

They are compared with results from a commercial code with a very refined mesh including 3800 dofs.

Only the more accurate model is assessed in this severe case. Figs. 16–18 show the in-plane, transverse displacements and in-plane, transverse shear and normal stresses along the thickness. The results perform very well with respect to the 2D reference solution. Note that the high variation of the transverse shear stress in the face is captured. For this case, only two couples are needed.

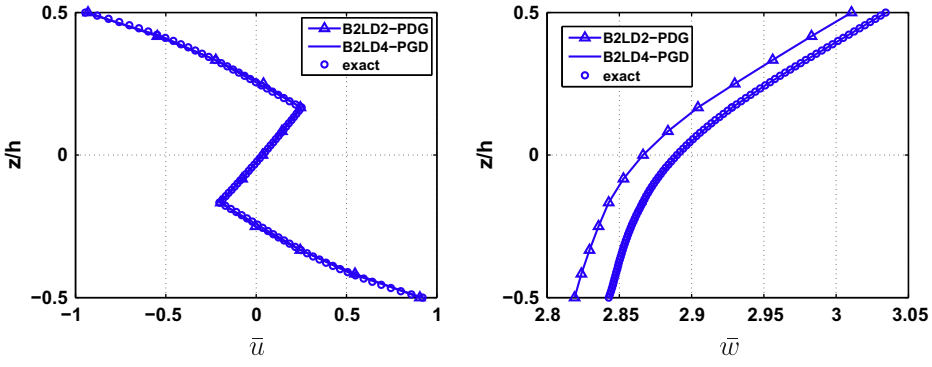

Fig. 12. Distribution of $\bar{u}$ (left) and $\bar{w}$ (right) along the thickness – $S = 4$ – 3 layers (0°/90°/0°) – $N_z = NC$.

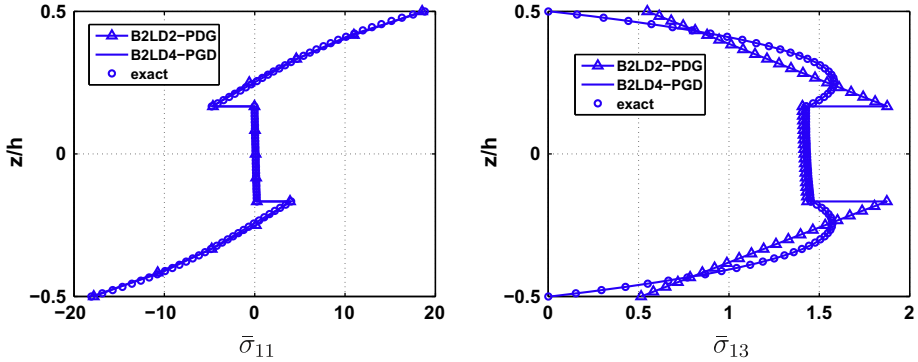

Fig. 13. Distribution of $\bar{\sigma}_{11}$ (left) and $\bar{\sigma}_{13}$ (right) along the thickness – $S = 4$ – 3 layers (0°/90°/0°) – $N_z = NC$.

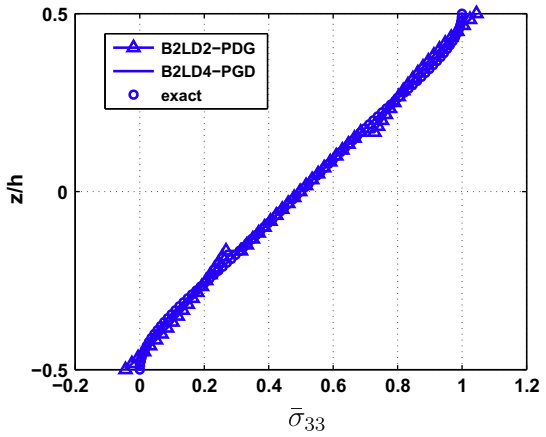

Fig. 14. Distribution of $\bar{\sigma}_{33}$ along the thickness – $S = 4$ – 3 layers (0°/90°/0°) – $N_z = NC$.

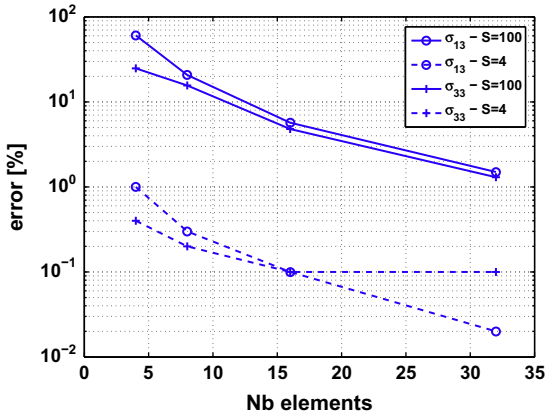

Fig. 15. Error on $\sigma_{13}(0,0)$ and $\sigma_{33}(L/2, h/2)$ with respect to the number of elements – $S = 4/100$ – 3 layers (0°/90°/0°) – $N_z = NC$.

The second mode is a local correction of the transverse normal stress in the faces of the sandwich beam. See Fig. 18.

5. Conclusion and future prospects

In this article, a beam finite element based on the PGD has been presented and evaluated through different benchmarks. This method has been applied to the modeling of both isotropic beam and laminated, sandwich composite. The displacement is expressed as a separated representation of two 1D functions. The axial functions have a parabolic distribution. For the transverse functions, a second and fourth-order expansion are considered. The derived iterative process implies the resolution of 1D problems and each of them has a low computational cost. The total cost depends on the number of couples necessary to represent the solution.

This study has showed the interesting capability of the method to build complex shape functions in the transverse direction, and to exhibit the main contributions of the z-expansion. This result depends on the complexity of the problem to be solved. This information is also the subject of a Carrera's work [43], dealing with the utmost terms as a function of the boundary conditions, the load, the slenderness ratio and the anisotropy. Several numerical evaluations have

Table 1
Two layers (0°/90°) – $N_x = 8$ sr (6) – $N_z = NC$.

S	Model	$\bar{u}(0, h/2)$	$\bar{w}(L, 0)$	$\bar{\sigma}_{11}(L/2, h/2)$	$\bar{\sigma}_{13}(0, -h/4)$
2	Exact	−0.7687	10.9008	1.4575	1.1637 (maxi)
	B2LD4-PGD	−0.7680 (0.1%)	10.8924 (0.1%)	1.4573 (0.0%)	1.1814 (1.5%)
4	Exact	−4.5680	4.7076	3.8377	2.7057
	B2LD4-PGD	−4.5680 (0.0%)	4.7077 (0.0%)	3.8393 (0.0%)	2.7342 (1.1%)
20	Exact	−486.3535	2.7092	76.6462	14.6209
	B2LD4-PGD	−486.4 (0.0%)	2.7079 (0.0%)	76.6840 (0.0%)	14.7460 (0.9%)
40	Exact	−3865.6117	2.6462	303.8544	29.3251
	B2LD4-PGD	−3865.8400 (0.0%)	2.6412 (0.2%)	304.0200 (0.1%)	30.2550 (3.2%)
100	Exact	−60288.9009	2.6285	1894.2817	73.3717
	B2LD4-PGD	−60289 (0.0%)	2.6150 (0.5%)	1895.4 (0.1%)	87.0610 (18.7%)

Table 2
Three layers (0°/90°/0°) – $N_x = 8$ – sr (6) – $N_z = NC$.

S	Model	$\bar{u}(0, h/2)$	$\bar{w}(L, 0)$	$\bar{\sigma}_{11}(L/2, h/2)$	$\bar{\sigma}_{13}(0, 0)$
2	Exact	−0.2216	8.5243	8.9546	0.5342
	B2LD4-PGD	−0.2216 (0.0%)	8.5240 (0.0%)	8.9547 (0.0%)	0.5342 (0.0%)
4	Exact	−0.9456	2.8899	18.8202	1.4319
	B2LD4-PGD	−0.9458 (0.0%)	2.8900 (0.0%)	18.8260 (0.0%)	1.4324 (0.0%)
20	Exact	−66.9407	0.6185	263.1638	8.7483
	B2LD4-PGD	−66.9500 (0.0%)	0.6185 (0.0%)	263.2600 (0.0%)	8.7593 (0.1%)
40	Exact	−519.1155	0.5379	1019.6788	17.6412
	B2LD4-PGD	−519.2 (0.0%)	0.5377 (0.0%)	1020.0 (0.0%)	17.7170 (0.4%)
100	Exact	−8038.4630	0.5152	6314.5597	44.2062
	B2LD4-PGD	8039.6 (0.0%)	0.5140 (0.2%)	6316.7 (0.0%)	45.3440 (2.6%)

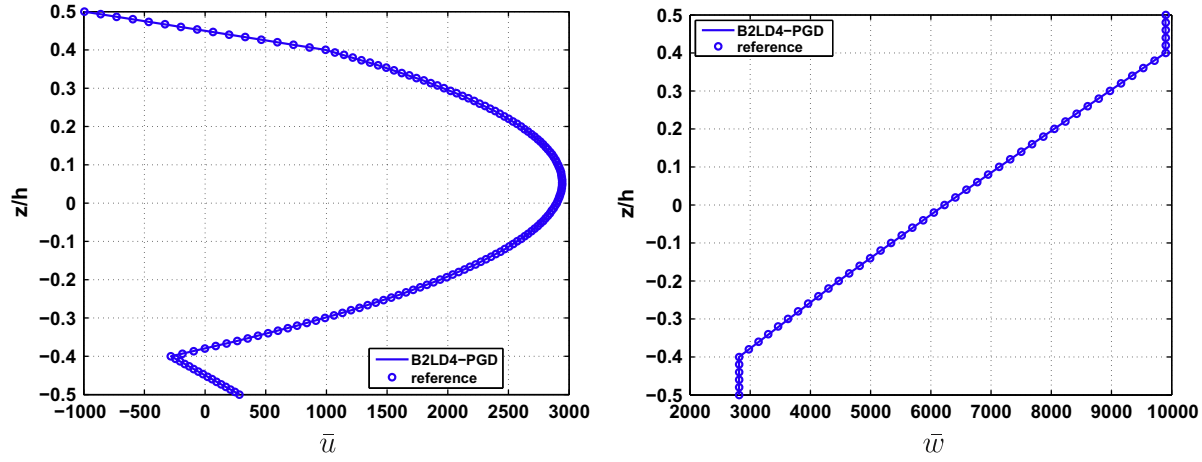

Fig. 16. Distribution of $\bar{u}$ (left) and $\bar{w}$ (right) along the thickness – $S = 4$ – sandwich – B2LD4-PGD.

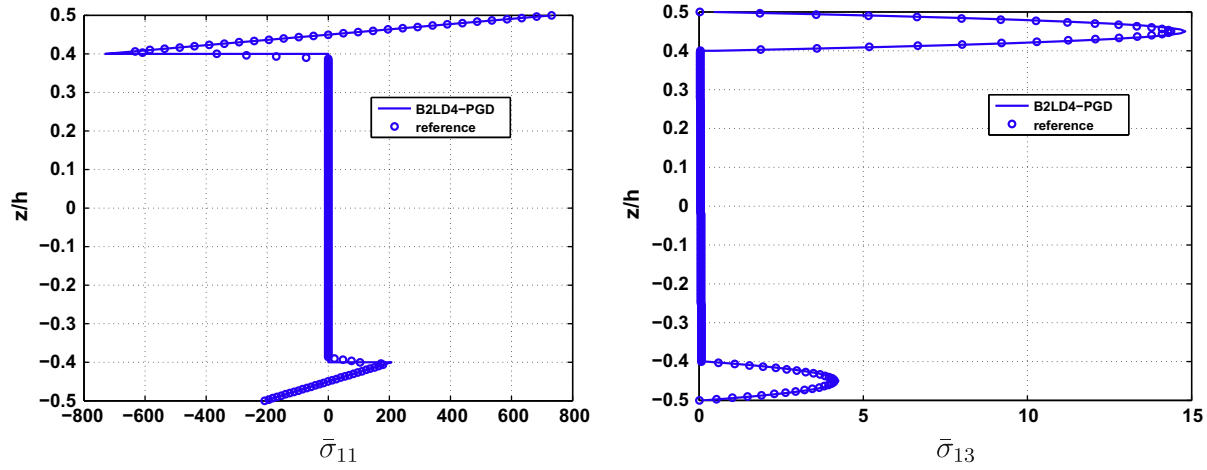

Fig. 17. Distribution of $\bar{\sigma}_{11}$ (left) and $\bar{\sigma}_{13}$ (right) along the thickness – $S = 4$ – sandwich – B2LD4-PGD.

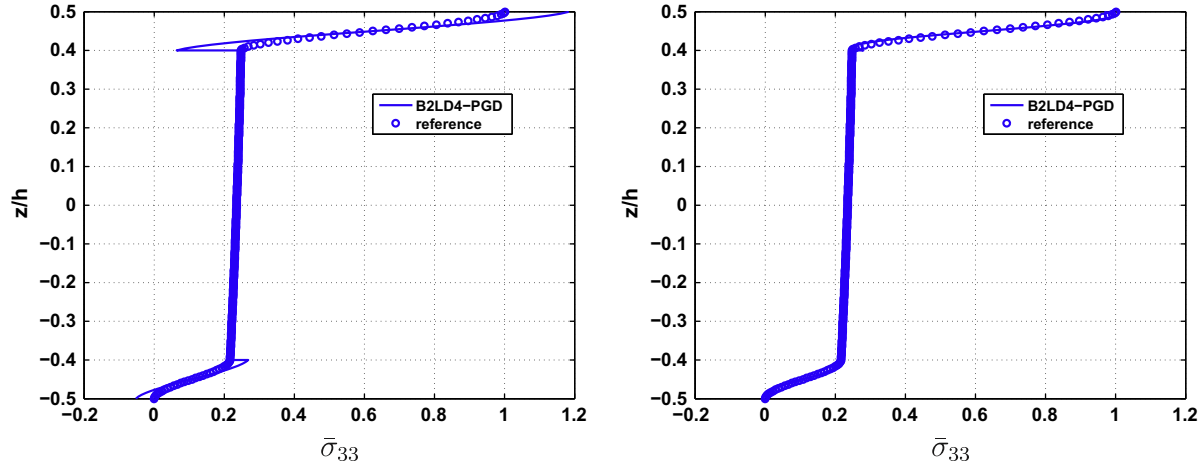

Fig. 18. Distribution of $\bar{\sigma}_{33}$ along the thickness – 1 couple (left) – 2 couples (right) – $S = 4$ – sandwich – B2LD4-PGD.

also proved that the fourth-order approach gives very accurate results and is suitable to model laminated and sandwich composite beam. Moreover, this approach is very interesting from a computational point of view, especially in the framework of LW approach.

Based on these promising results, the use of PGD for plate and shell structures will be carried out.

References

[1] Tanigawa Y, Murakami H, Ootao Y. Transient thermal stress analysis of a laminated composite beam. J Therm Stresses 1989;12:25–39.
[2] Yang P, Norris C, Stavsky Y. Elastic wave propagation in heterogeneous plates. Int J Solids Struct 1966;2:665–84.
[3] Librescu L. On the theory of anisotropic elastic shells and plates. Int J Solids Struct 1967;3:53–68.
[4] Whitney J, Sun C. A higher order theory for extensional motion of laminated composites. J Sound Vibr 1973;30:85–97.
[5] Lo K, Christensen R, Wu F. A higher-order theory of plate deformation. Part II: Laminated plates. J Appl Mech ASME 1977;44:669–76.
[6] Reddy J. A simple higher-order theory for laminated composite plates. J Appl Mech ASME 1984;51(4):745–52.
[7] Matsunaga H. Assessment of a global higher-order deformation theory for laminated composite and sandwich plates. Compos Struct 2002;56:279–91.
[8] Kant T, Swaminathan K. Analytical solutions for the static analysis of laminated composite and sandwich plates based on a higher order refined theory. Compos Struct 2002;56:329–44.
[9] Cook G, Tessler A. A {3,2}-order bending theory for laminated composite and sandwich beams. Compos Part B: Eng J 1998;29B:565–76.
[10] Carrera E. A priori vs. a posteriori evaluation of transverse stresses in multilayered orthotropic plates. Compos Struct 2000;48(4):245–60.
[11] Kim J-S, Cho M. Enhanced first-order theory based on mixed formulation and transverse normal effect. Int J Solids Struct 2007;44:1256–76.
[12] Heller R, Swift G. Solutions for the multilayer timoshenko beam. In: Report N VPI-E-71-12, Virginia Polytechnic Institute, Blacksburg, VA; 1971.
[13] Swift G, Heller R. Layered beam analysis. J Eng Mech ASCE 1974;100:267–82.
[14] Srinivas S. A refined analysis of laminated composites. J Sound Vibr 1973:495–507.
[15] Whitney J. The effect of transverse shear deformation in the bending of laminated plates. J Compos Mater 1969;3:534–47.
[16] Pagano N. Exact solutions for composite laminates in cylindrical bending. J Compos Mater 1969;3:398–411.
[17] Shimpi R, Ainapure A. A beam finite element based on layerwise trigonometric shear deformation theory. Compos Struct 2001;53:153–62.
[18] Reddy J. On refined computational models of composite laminates. Int J Numer Meth Eng 1989;27:361–82.
[19] Ferreira A. Analysis of composite plates using a layerwise shear deformation theory and multiquadrics discretization. Mech Adv Mater Struct 2005;12:99–112.
[20] Icardi U. Higher-order zig-zag model for analysis of thick composite beams with inclusion of transverse normal stress and sublaminates approximations. Compos Part B: Eng J 2001;32:343–54.
[21] Rao M, Desai Y. Analytical solutions for vibrations of laminated and sandwich plates using mixed theory. Compos Struct 2004;63:361–73.
[22] Carrera E. A study of transverse normal stress effect on vibration of multilayered plates and shells. J Sound Vibr 1999;225:803–29.
[23] Ambartsumyan S. Theory of anisotropic plates. Technomic Publishing Co.; 1969 [translated from russian by T. Cheron and Edited by J.E. Ashton].
[24] Lee C-Y, Liu D, Lu X. Static and vibration analysis of laminated composite beams with an interlaminar shear stress continuity theory. Int J Numer Meth Eng 1992;33:409–24.
[25] Sciuva MD, Icardi U. Numerical assessment of the core deformability effect on the behavior of sandwich beams. Compos Struct 2001;52:41–53.
[26] Kapuria S, Dumir P, Ahmed A. An efficient higher order zigzag theory for composite and sandwich beams subjected to thermal loading. Int J Solids Struct 2003;40:6613–31.
[27] Vidal P, Polit O. A family of sinus finite elements for the analysis of rectangular laminated beams. Compos Struct 2008;84:56–72. doi:10.1016/j.compstruct.2007.06.009.
[28] Vidal P, Polit O. A refined sine-based finite element with transverse normal deformation for the analysis of laminated beams under thermomechanical loads. J Mech Mater Struct 2009;4(6):1127–55.
[29] Vidal P, Polit O. A sine finite element using a zig-zag function for the analysis of laminated composite beams. Compos Part B: Eng J 2011;42(6):1671–82. doi:10.1016/j.compositesb.2011.03.012.
[30] Noor A, Burton W. Assessment of computational models for multilayered composite shells. Appl Mech Rev 1990;43(4):67–97.
[31] Reddy J. Mechanics of laminated composite plates – theory and analysis. Boca Raton (FL): CRC Press; 1997.
[32] Carrera E. Theories and finite elements for multilayered, anisotropic, composite plates and shells. Arch Comput Meth Eng 2002;9:87–140.
[33] Carrera E. Historical review of zig-zag theories for multilayered plates and shells. Appl Mech Rev 2003;56(3):287–308.
[34] Zhang Y, Yang C. Recent developments in finite elements analysis for laminated composite plates. Compos Struct 2009;88:147–57.
[35] Ammar A, Mokdada B, Chinesta F, Keunings R. A new family of solvers for some classes of multidimensional partial differential equations encountered in kinetic theory modeling of complex fluids. J Non-Newton Fluid Mech 2006;139:153–76.
[36] Ladevèze P. Nonlinear computational structural mechanics – new approaches and non-incremental methods of calculation. Springer-Verlag; 1999.
[37] Allix O, Vidal P. A new multi-solution approach suitable for structural identification problems. Comput Methods Appl Mech Eng 2002;191(25–26):2727–58.
[38] Bognet B, Bordeu F, Chinesta F, Leygue A, Poitou A. Advanced simulation of models defined in plate geometries: 3d solutions with 2d computational complexity. Comput Methods Appl Mech Eng; in press. doi:10.1016/j.cma.2011.08.025.
[39] Nouy A. A priori model reduction through proper generalized decomposition for solving time-dependent partial differential equations. Comput Methods Appl Mech Eng 2010;199(23–24):1603–26.
[40] Chinesta F, Ammar A, Leygue A, Keunings R. An overview of the proper generalized decomposition with applications in computational rheology. J Non-Newton Fluid Mech 2011;166(11):578–92.
[41] Polit O, Vidal P, D'Ottavio M. Robust c^0 high-order plate finite element for thin to very thick structures: mechanical and thermo-mechanical analysis. Int J Numer Meth Eng 2012. in press.
[42] Brischetto S, Carrera E, Demasi L. Improved bending analysis of sandwich plates using zig-zag function. Compos Struct 2009;89:408–15.
[43] Carrera E, Miglioretti F, Petrolo M. Accuracy of refined finite elements for laminated plate analysis. Compos Struct 2011;93:1311–27.